34th Annual International Conference of the IEEE EMBS
San Diego, California USA, 28 August - 1 September, 2012

Carotid Ultrasound Symptomatology using Atherosclerotic Plaque Characterization: A class of Atheromatic Systems

U Rajendra Acharya, Vinitha Sree S*, Filippo Molinari, Luca Saba,

Andrew Nicolaides, Shoaib Shafique, Jasjit S Suri**, Fellow AIMBE

***Abstract*— In this paper, we present a Computer Aided Diagnosis (CAD) based technique (Atheromatic system) for classification of carotid plaques in B-mode ultrasound images into symptomatic or asymptomatic classes. This system, called Atheromatic, has two steps: (i) feature extraction using a combination of Discrete Wavelet Transform (DWT) and averaging algorithms and (ii) classification using Support Vector Machine (SVM) classifier for automated decision making. The CAD system was built and tested using a database consisting of 150 asymptomatic and 196 symptomatic plaque regions of interests which were manually segmented. The ground truth of each plaque was determined based on the presence or absence of symptoms. Three-fold cross-validation protocol was adapted for developing and testing the classifiers. The SVM classifier with a polynomial kernel of order 2 recorded the highest classification accuracy of 83.7%. In the clinical scenario, such a technique, after much more validation, can be used as an adjunct tool to aid physicians by giving a second opinion on the nature of the plaque (symptomatic/ asymptomatic) which would help in the more confident determination of the subsequent treatment regime for the patient.**

***Index Terms*—Atherosclerosis, Carotid ultrasound, Grayscale Features, Discrete Wavelet Transform, Support Vector Machine (SVM), classification.**

I. Introduction

Deposition of plaques results in thickening of arteries and leads to atherosclerosis [1]. Atherosclerosis is a common disease, and hence, a diagnosis support system must be economical in order to keep the financial burden on society as low as possible. It has been observed that symptomatic patients (who have had retinal or hemispheric symptoms such as stroke, Transient Ischemic Attack (TIA), and Amaurosis Fugax (AF)) have more frequent plaque ruptures that cause life-threatening embolization. Plaque rupture was seen in 74% of symptomatic plaques and in only 32% of plaques from asymptomatic patients [2]. Since there is a considerable risk for the patient undergoing Carotid Artery Stenting (CAS) and Carotid Endarterectomy (CEA), techniques are needed to effectively select only those symptomatic patients at risk of stroke for these procedures.

Ultrasound imaging is cost effective and affordable, and hence, is a good choice for medical data acquisition. It was shown that ultrasonographic B-mode characterization of plaque morphology may be useful in the assessment of the atherosclerotic lesion vulnerability [3]. In spite of significant advantages of diagnostic ultrasound, it is limited by low spatial resolution and artifacts [4]. Hence, improvement of ultrasonographic image quality using adequate image pre-processing techniques and extraction of good features may improve its diagnostic accuracy.

In this work, we present a low-cost non-invasive Computer-Aided Diagnosis (CAD) system that uses image processing and data mining techniques for classifying symptomatic and asymptomatic plaques. We call this as a class of Atheromatic systems. Important salient features are extracted from the B-mode ultrasound images using Discrete Wavelet Transform (DWT) and fed to the Support Vector Machine (SVM) classifier for automated classification.

II. Materials and Methods

Fig. 1 shows the block diagram of the proposed Atheromatic class of system. The ultrasound images of carotid plaque are pre-processed and subjected to feature extraction using DWT technique. Subsequently, the significant features are extracted using Student's *t*-test. Selected features are then fed to the SVM classifier for classification.

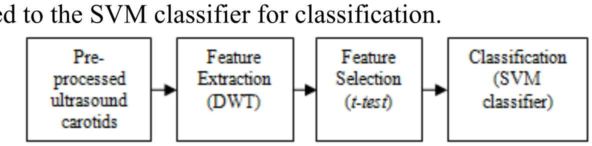

Fig. 1. Block diagram of the Atheromatic Class of system.

A. *Ultrasound Images of Carotid Plaque*

We used 150 asymptomatic and 196 symptomatic (a total of 346) carotid plaque ultrasound images. These images were collected from patients referred to the Vascular Screening Diagnostic Center, Nicosia, Cyprus, for diagnostic carotid ultrasound to detect both presence and severity of internal carotid stenosis. Approval from Institutional Review

Manuscript received January 26, 2012.

U. Rajendra Acharya is with the Department of Electronics and Computer Engineering, Ngee Ann Polytechnic, Singapore

Vinitha Sree is with Global Biomedical Technologies Inc., CA, USA (email: vinitha.sree@gmail.com)

Filippo Molinari is with Biolab, Department of Electronics and Telecommunications, Politecnico di Torino, Torino, Italy.

Luca Saba is with the Department of Radiology, Azienda Ospedaliero Universitaria di Cagliari, Cagliari, Italy

Andrew Nicolaides is with the Vascular Screening and Diagnostic Centre, London, and Department of Biological Sciences, University of Cyprus, Nicosia, Cyprus

Shoaib Shafique, MD, is with CorVas, West Lafayette, Indiana, USA.

**Jasjit S. Suri, Fellow AIMBE, is a CTO with Global Biomedical Technologies, CA, USA and is also affiliated with Biomedical Engineering Department, Idaho State University, ID, USA (jsuri@comcast.com). All questions to be addressed to.

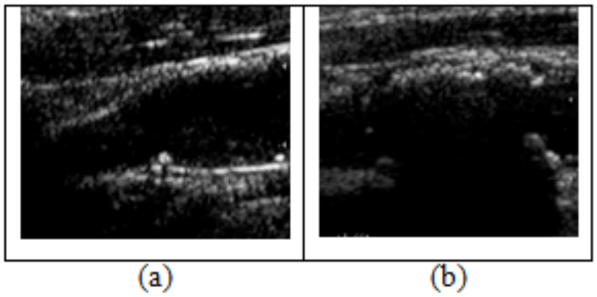

Fig. 2. Carotid images: (a) Symptomatic (AF) (b) Asymptomatic (AS).

Board and consent from patients were obtained prior to conducting the study. Subjects with cardioembolic symptoms or distant symptoms (> six months) were not included in this work. The plaques with less than 50% stenosis were not included in the database [5]. In order to ensure that images acquired under different conditions produce comparable and reproducible features and classification, image normalization was carried out using the technique reported in [6]. The gray scale images were normalized (using blood and adventitia as reference points) manually by adjusting the image linearly so that the median gray level value of blood was in the range of 0–5, and the median gray level of adventitia (artery wall) was in the range of 180–190.

There were 196 symptomatic plaques (88 stroke, 70 TIA, and 38 AF). Asymptomatic plaques were from patients who had no symptoms in the past. During pre-processing, the Region of Interest (ROI) was manually segmented by medical practitioner from each of the studied images prior to feature extraction. The nature of the disease is focused on the vessel wall that specifically changes the morphology of the lumen-intima interface from slow gradual lipid formation and maturing into hard plaque or loose island of haemorrhage [7]. Thus, the young and old plaques are all focused towards the vessel disease which yields the information in the form of echogenicity in the ultrasound image [8]. Therefore, the focused ROI constitutes less than 25% of the image frame, and hence, the vascular surgeons are keenly interested in characterization of plaque in this regional information. We are therefore focused in this paper in analyzing the small ROI traced by the vascular surgeon. Typical symptomatic and asymptomatic carotid images are shown in Fig. 2(a) and Fig. 2(b). Fig. 3(a) and Fig. 3(b) show the ROIs of symptomatic and asymptomatic carotid images.

A. Feature Extraction

The DWT transform of a signal x is determined by sending the signal through a sequence of down-sampling high and low pass filters. The low pass filter is defined by the transfer function $g[n]$ and the high pass filter by the transfer function $h[n]$. The output of the high pass filter $D[n]$ is known as the detail coefficients. The output of the low pass filter is known as the approximation coefficients. Specifically, we used Wavelet packets in this work. The images are represented as an m x n gray scale matrix $I[i, j]$ where each element of the matrix represents the intensity of one pixel. There were four possible decompositions corresponding to 0° (horizontal, Dh), 90° (vertical, Dv) and 45° or 135° (diagonal, Dd) orientations (Fig. 4). The diagram shows the $N \times M$ dimensional input image $I[i, j]$ and the results for level 1. In this work, we found that the results from level 1 were sufficient to obtain significant features.

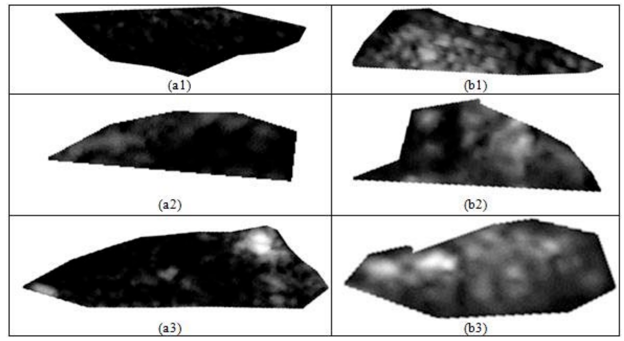

Fig. 3. Region of interest extracted from the carotid plaque ultrasound images of (a) Symptomatic (AF) and (b) Asymptomatic (AS) patients.

The first level 2D DWT yields four result matrices, namely Dh_1, Dv_1, Dd_1 *and* A_1, whose elements are intensity values. Unfortunately, these matrixes cannot be used for classification directly, because the number of elements is too high. Therefore, we defined two averaging methods which represent result matrixes with just one number. The first method is used to extract average measures from 2D DWT result vectors.

$$Average\ Dh_1\ (Ah) = \frac{1}{N \times M} \sum_{x=<N>} \sum_{y=<M>} \left| Dh_1(x,y) \right| \tag{1}$$

$$Average\ Dv_1\ (Av) = \frac{1}{N \times M} \sum_{x=<N>} \sum_{y=<M>} \left| Dv_1(x,y) \right| \tag{2}$$

The final averaging method uses average of the energy of the intensity values.

$$Energy\ (E) = \frac{1}{N^2 \times M^2} \sum_{x=<N>} \sum_{y=<M>} \left(Dv_1(x,y) \right)^2 \tag{3}$$

These three elements form the feature vector.

B. Support Vector Machine

SVM is a hyperplane-based nonparametric classifier. When it is trained using input features-output ground truth class label pairs, it outputs a decision function which can be used to test new input features. Assuming that the class label c = -1 for asymptomatic class and +1 for symptomatic class, the SVM algorithm maps the training set into a feature space and attempts to locate in that space a hyperplane that separates the positive from the negative examples. During the testing of an unlabelled sample, the algorithm maps the sample into the same feature space and determines its class

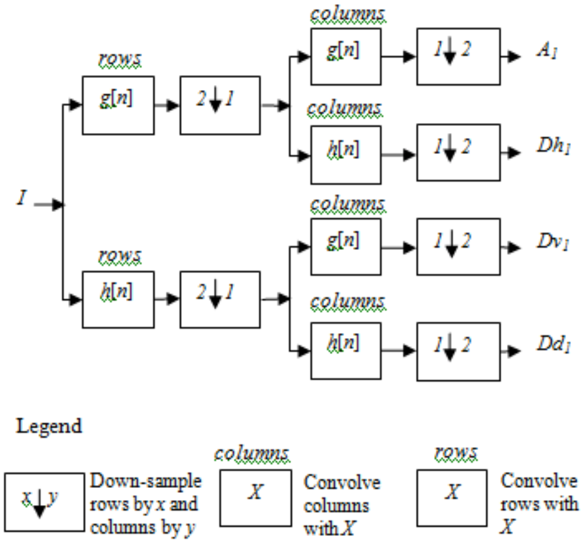

Fig. 4. Discrete Wavelet Transform (DWT) decomposition.

based on which side of the separating plane the sample is present. Thus, the main objective of SVM is to determine a separating hyperplane that maximizes the margin between the input data classes which are plotted in the feature space [9]. In the case of linearly non-separable data, the features are first mapped to a higher dimensional space using kernel functions [10], and then the hyperplane is determined.

III. Results

A. Selected Features

In this work, we compared the performance of 54 different wavelet functions. The mother wavelet families that were analyzed were Reverse Biorthogonal wavelet family (*rbio*), Daubechies wavelet (*db*), Biorthogonal 3.1 wavelet (*bior*), Coiflets, Symlets, Discrete Meyer (FIR approximation) (*dmey*) and Haar family. The biorthogonal (*bior3.1*) performed better compared to the other wavelet functions. We have used t-test [11] to verify if the features are significant enough to be able to accurately discriminate the symptomatic and asymptomatic classes. A p-value of less than 0.0001 indicates that the features are significant. The features selected were: energy, average horizontal and vertical DWT coefficients. Table I presents the features obtained using DWT with the bior3.1 wavelet.

TABLE I
FEATURES OBTAINED USING THE DISCRETE WAVELET TRANSFORM (DWT) METHOD USING BIOR3.1 WAVELET FUNCTION

Feature	Asymptomatic	Symptomatic	*p*-value
Average Dh_1 *(Ah)*	0.10 ± 0.04	0.14 ± 0.03	< 0.0001
Average Dv_1 *(Av)*	3.82E-02 ± 1.55E-02	5.49E-02 ± 1.47E-02	< 0.0001
Energy (E)	5.47E-08 ± 2.22E-08	7.17E-08 ± 1.99E-08	< 0.0001

B. Classification Results

Three-fold stratified cross validation method was used to evaluate these classifiers. In this method, the dataset of 346 images was split into three parts, each part containing the same proportion of images from both classes. In the first fold, two parts were used for training and the third part was used for testing and for calculation of the performance measures. This protocol was repeated two more times with a different part as the test set. The averages of the performance measures (sensitivity, specificity, Positive Predictive Value (PPV), and accuracy) obtained during the testing phase of each fold are reported as the final performance measures for that classifier. Since SVM performed better among the 15 classifiers used, we have shown the performance measures obtained using various kernel configurations in Table II. Sensitivity is the probability that the technique will identify symptomatic cases, and specificity is the probability that the technique will identify asymptomatic cases. PPV is the proportion of symptomatic subjects among those who were labeled symptomatic by the technique, and accuracy is the ratio of the number of correctly classified samples to the total number of samples. Our results show that the SVM classifier with the polynomial kernel of order 2 achieved an average accuracy of 83.7%, sensitivity of 80%, specificity of 86.4%, and PPV of 81.8%.

TABLE II
CLASSIFICATION RESULTS OBTAINED USING THE DWT FEATURES IN THE VARIOUS CONFIGURATIONS OF THE SUPPORT VECTOR MACHINE (SVM) CLASSIFIER; A: ACCURACY; SN: SENSITIVITY; SP: SPECIFICITY

SVM	A (%)	PPV (%)	Sn (%)	Sp (%)
Linear	81.7	77	82.2	81.3
Polynomial order 1	81.7	77	82.2	81.3
Polynomial order 2	83.7	81.8	80	86.4
Polynomial order 3	82.6	84.6	73.3	89.8
RBF	80.8	79	75.5	84.7

IV. Discussion

A scale/frequency approach was used to characterize carotid atherosclerotic plaque from B-mode ultrasound [12]. It was shown that WP analysis by the use of Haar filter and the 1-1 norm as texture descriptor could reveal differences not only in high but also in low frequencies, and therefore, could characterize efficiently the atheromatous tissue. Normalized pattern spectra computed for both a structural, multilevel binary morphological model were used as classification features to obtain an accuracy of 73.7% using the SVM classifier [13]. The texture and motion patterns of carotid atherosclerosis features were extracted and fed to a fuzzy C-means classifier to present an accuracy of 84% [14]. It was shown that Gabor filter-based texture analysis in combination with bootstrapping may provide valuable information to discriminate the two plaque tissue types [15]. In another study [16], 61 texture and shape features from manually segmented plaque ROIs were used in a modular neural network and an accuracy of 73.1% was reported.

It is evident from the above discussed studies that there is a need for techniques that are more accurate and that use lesser number of features. Since most of these studies employ texture features in our earlier work [17], we evaluated the same dataset used in this work using texture features coupled with SVM and obtained the highest classification accuracy of 82.4%. In order to improve the accuracy further, in this work, we decided to study the capability of DWT based features for the plaque classification problem. Our proposed method resulted in accuracy, sensitivity, and specificity of 83.7%, 80%, and 86.4%, respectively. The key features of the proposed Atheromatic Class of system are summarized below:

[a] The feature set is small (only three features), and yet is powerful enough to effectively classify symptomatic and asymptomatic plaques with good accuracy of 83.7%.

[b] The technique is robust as we have evaluated it using a large database (150 asymptomatic and 196 symptomatic plaques) using three-fold cross validation technique.

[c] The system is real-time as no manual interaction is necessary except for the selection of the ROI.

[d] The accuracy of our work is relatively higher than that reported by previous studies. The proposed technique can thus serve as an adjunct tool to give the physician a valuable second opinion on treatment selection.

[e] The technique is low cost as it uses features extracted from the ultrasound image and there is absolutely no cost needed for deployment in the doctor's office.

We do however believe that there is a scope of improving the efficiency by adding more advanced features which can represent atherosclerotic deposits in wall region and our group is committed towards improving this system for next generation. In future, hope that the ROI segmentation can potentially be done automatically. A drawback of the ground truth determination based on presence or absence of symptoms is that some of the asymptomatic plaques might have been wrongly labelled as symptomatic when the symptoms might have occurred due to plaque in heart and not in the carotid artery. Also, patients who do not recollect their history of symptoms may be classified as asymptomatic. To alleviate this problem, in our future studies, we intend to determine the ground truth from pathological studies on the plaque instead of from the clinical report on the patient's symptoms.

V. Conclusion

In this work, we have presented a CAD tool called Atheromatic system for carotid plaque characterization and classification into symptomatic and asymptomatic classes. Our system uses DWT for feature extraction and can diagnose the two classes automatically with an accuracy, sensitivity and specificity of more than 83%. This accuracy is relatively higher than those recorded in similar studies in the literature. Hence, we believe that the proposed technique can be considered as an ***effective image mining technique*** which can serve as an efficient adjunct tool for the vascular surgeons in selecting patients for risky stenosis treatments. However, these accuracies may not be sufficient enough for the system to be incorporated into routine clinical work flow. Therefore, in the future, we intend to study different features such as a combination of texture and DWT features to improve the diagnostic accuracy.

References

[1] A. Maton, J. Hopkins, C. W. McLaughlin, S. Johnson, M. Q. Warner, D. LaHart, and J. D. Wright, Human Biology and Health. New Jersey, USA: Prentice Hall, 1993.

[2] S. Carr, A. Farb, W. H. Pearce, R. Virmani, and J. S. Yao, "Atherosclerotic plaque rupture in symptomatic carotid artery stenosis," *J. Vasc. Surg.,* vol. 23, no. 5, pp. 755-765, May 1996.

[3] A. F. AbuRahma, J. Wulu, John T., and B. Crotty, "Carotid plaque ultrasonic heterogeneity and severity of stenosis," *Stroke*, vol. 33, no. 7, pp.1772–1775, Jul. 2002.

[4] D. W. Droste, M. Karl, R. M. Bohle, and K. M, "Comparison of ultrasonic and histopathological features of carotid artery stenosis," Neurol. Res., vol. 19, pp. 380 – 384, Aug. 1997.

[5] European Carotid Surgery Trialists' Collaborative Group. Randomised trial of endarterectomy for recently symptomatic carotid stenosis: Final results of the MRC European Carotid Surgery Trial (ECST). *Lancet*, vol. 351, no. 9113, pp. 1379–1387, May 1998.

[6] T. Elatrozy, A. Nicolaides, T. Tegos, and M. Griffin, "The objective characterization of ultrasonic carotid plaque features," *Eur. J. Vasc. Endovasc. Surg.,* vol. 16, no. 3, pp. 223-230, Sep. 1998.

[7] N. Carter-Monroe, S. K. Yazdani, E. Ladich, F. D. Kolodgie and R. Virmani, Introduction to the Pathology of Carotid Atherosclerosis: Histologic Classification and Imaging Correlation, in *Atherosclerosis Disease Management*, 2011, Part 1, pp. 3-35.

[8] M. B. Griffin, E. Kyriacou, C. Pattichis, D. Bond, S. K. Kakkos, M. Sabetai, G. Geroulakos, N. Georgiou, C. J. Dore, and A. Nicolaides, "Juxtaluminal hypoechoic area in ultrasonic images of carotid plaques and hemispheric symptoms," *J. Vasc. Surg*., vol. 52, no. 1, pp. 69-76, Jul. 2010

[9] V. Vapnik, *Statistical Learning Theory*. New York: Wiley, 1998.

[10] V. David and A. Sanchez, "Advanced support vector machines and kernel methods," *Neurocomputing*, Elsevier, 2003.

[11] J. F. Box, "Guinness, gosset, fisher, and small samples," *Statist. Sci.*, vol. 2, no. 1, pp. 45–52, 1987.

[12] N. Tsiaparas, S. Golemati, J. Stoitsis, and K. S. Nikita, "Discrete wavelet transform vs. wavelet packets for texture analysis of ultrasound images of carotid atherosclerosis," *Proc. 9th Int;. Conf. Information Technology and Applications in Biomedicine*, pp. 1-4, 2009.

[13] E. Kyriacou, M. Pattichis, C. S. Pattichis, A. Mavrommatis, C. I. Christodoulou, S. Kakkos, and A. Nicolaides, "Classification of atherosclerotic carotid plaques using morphological analysis on ultrasound images," *J. Appl. Intell.*, vol. 30, no. 1, pp. 3–23, 2009.

[14] J. Stoitsis, S. Golemati, K. S. Nikita, and A.N. Nicolaides, "Characterization of carotid atherosclerosis based on motion and texture features and clustering using fuzzy c-means," *Proc. 26th Annu. Intl. Conf. IEEE EMBS*, San Francisco, CA, USA, pp. 1407-1410, 2004.

[15] J. Stoitsis, S. Golemati, N. Tsiaparas, K. S. Nikita, "Texture characterization of carotid atherosclerotic plaque from bmode ultrasound using Gabor filters" *Proc. 31st Annu. Intl. Conf. IEEE EMBS*, Minneapolis, Minnesota, USA, pp. 455-458, 2009.

[16] C. I. Christodoulou, C. S. Pattichis, M. Pantziaris, and A. Nicolaides, "Texture based classification of atherosclerotic carotid plaques," *IEEE Trans. Med. Imaging*, vol. 22, no. 7, pp. 902–912, 2003.

[17] R. U. Acharya, O. Faust, A. P. Alvin, S. Vinitha Sree, F. Molinari, L. Saba, A. Nicolaides, and J. S. Suri, "Symptomatic vs. asymptomatic plaque classification in carotid ultrasound," *J. Med. Syst.*, Jan 2011. DOI: 10.1007/s10916-010-9645-2.